MINIATURIZED ULTRAWIDEBAND WIDE SLOT ANTENNA WITH DUAL BAND-NOTCHES AND ELIMINATING SPURIOUS STOP BAND

Z.-M. Yan, Y.-S. Xu[*], and W.-D. Wang

Department of Electronic Engineering and Information Science, University of Science and Technology of China, Hefei, Anhui 230027, China

Abstract—A wide slot antenna fed by a microstrip line ended with a hexagonal tuning stub and its variation with dual band-notched function for ultrawideband operations are presented. The fundamental configuration is a rectangular slot on a printed circuit board with a low relative dielectric constant of 2.65. Three tuning stubs are employed at the edges of the slot to ensure the impedance matching. This original antenna achieves an operation bandwidth from 3.1 to 11.5 GHz with a stable gain performance and a very compact size of 22 mm × 22 mm × 0.5 mm. By etching a C-shaped slit and a Hilbert fractal curve slit on the original antenna without retuning, band-notched characteristics in the 3.40–3.69 GHz WiMAX band and the 5.15–5.825 GHz WLAN band can be realized, respectively. A rectangular patch is added to eliminate the spurious notched band around 10.5 GHz.

1. INTRODUCTION

In 2002, the Federal Communications Commission of the USA released the unlicensed use of the frequency spectrum from 3.1 to 10.6 GHz for ultrawideband (UWB) applications. For compact UWB systems, low profile is a very important issue. With the enormous progress in very large scale integration technology, the portable wireless devices become much smaller than before and the antennas become one of the bottlenecks in the miniaturization of portable devices.

Printed wide slot antennas are good choices to overcome the above difficulty because of their small sizes, ease of fabrication, wide

bandwidth, and steady radiation patterns. Recently, slot antennas of various shapes have been proposed [1–8].

Because of the existence of other wireless systems, such as wireless local area network (WLAN) and worldwide interoperability for microwave access (WiMAX), an additional requirement for UWB antennas is to construct some notched bands within the passband to avoid interference. The 3.5 GHz band (3.40–3.69 GHz) for the WiMAX and 5.5 GHz band (5.15–5.825 GHz) for the WLAN should be notched in the antenna design [2]. Many schemes have been proposed to realize band-notched performances [2–14], such as inserting two symmetric open-circuited stubs [5], quarter wavelength slits [6, 7] or stubs [8], a pair of coupled lines [9], or parasitic elements [10, 11].

This wok presents a microstrip-fed rectangular wide slot antenna with rectangular and hexagonal tuning stubs at the edges of the slot and the end of the microstrip line, respectively. Fabricated on a printed circuit board with low relative dielectric constant of 2.65, the antenna has a very compact size of 22 mm × 22 mm × 0.5 mm and covers the band of 3.1–11.5 GHz. A Hilbert fractal curve slit and a C-shaped slit are etched on the hexagonal tuning stub of the original antenna and on the ground to obtain dual band-notches around 5.5 and 3.5 GHz, respectively. The fractal curve slit can achieve a sharper band-notched characteristic with a more compact structure. Theoretically, the stop band caused by a band-notch slit appears periodically as the frequency arises due to its resonance nature. Higher frequency stop bands, namely spurious stop bands, are likely to fall in the operation band. This kind of spurious stop bands is observed in [12] and they are caused by the high order harmonics of the slit structures. In [13], the concentration and resonance of the current around the band-notch strip at the second harmonic frequency 11 GHz are also reported. In general, however, such a subject is rarely or not in detail addressed in the published literature. When a spurious stop band falls in the operation band and its effect is so significant such that it deteriorates the matching performance obviously and cannot be attenuated to an acceptable level by simple parametric study in the design procedures, further design considerations are then needed. This is exactly situation for the 3.5 GHz notched band in the present work. We propose a new scheme to eliminate the spurious notched band around 10.5 GHz. A rectangular patch resonating and radiating in the same frequency range is added to compensate for the mismatch caused by the non-radiating resonance slit.

2. ANTENNA CONFIGURATION AND DESIGN

2.1. Fundamental Antenna Configuration

A fundamental antenna configuration is shown in Figures 1(a) and 1(b). The substrate material consists of two metallic layers on a printed circuit board with relative dielectric constant 2.65. The width L_x, length L_y, and thickness h of the substrate are 22 mm, 22 mm, and 0.5 mm, respectively. A wide slot is etched on the bottom or ground layer as a radiating element and fed by a 50 Ω microstrip line of width $w = 1.35$ mm and length $f_\ell = 4.0$ mm on the top layer. A widened hexagonal feeding stub of width w_f and length ℓ_f is connected to the end of the microstrip line to obtain better impedance matching. The spacing s between the feeding stub and the lower edge of the wide slot and the height t of the slope are important parameters for the matching performance over the entire band. The wide slot on the bottom layer is a rectangle of width W_x and length W_y. A rectangular stub of width w_t and length d is added to the upper edge of the slot. This stub introduces additional capacitance between the feeding line and the ground plane and is intended to extend the lower edge operation frequency. The two symmetrically placed rectangular stubs of width s_x and length s_y at the lower edge of the slot, separated by a distance of $2d_t$, improve impedance matching at higher frequencies.

2.2. UWB Antenna without Band-notch

The proposed antenna without any band-notch has already been depicted in Figures 1(a) and 1(b). Parametric studies have been carried out to achieve desired performance. The simulations are performed using Ansoft HFSS and a SMA connector together with a 30.0 mm long straight coaxial line is included in the simulation model. The SMA connector can be considered as an extension of the ground plane and has slight effect on the lower edge frequency of the compact antenna. The wide band performance is sensitive to the dimensions of the tuning stubs at the edges of the wide slot.

The operation band of a conventional rectangular wide slot antenna is mainly affected by the slot width and length. Size reduction of the conventional antenna shifts the lowest resonance frequency to a higher frequency point. Our design aims to realize antenna miniaturization while preserving the desired UWB bandwidth. The rectangular tuning stub attached to the upper edge of the wide slot serves mainly for this purpose. The stub increases the total perimetric length of the slot and prolongs actually the path of the current flow along the slot edge, such that a resonance around the lower UWB
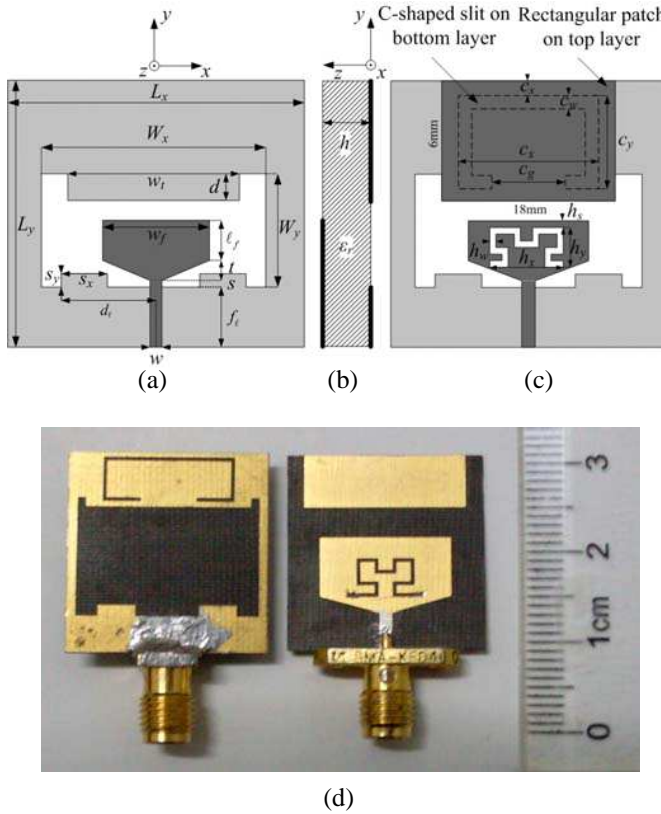
(a)   (b)   (c)

(d)

Figure 1. Antenna structures. (a) Fundamental antenna configuration without band-notches. $\varepsilon_r = 2.65$, $h = 0.5\,\text{mm}$, $w = 1.35\,\text{mm}$, $L_x = 22.0\,\text{mm}$, $L_y = 22.0\,\text{mm}$, $W_x = 20.0\,\text{mm}$, $W_y = 13.0\,\text{mm}$, $f_\ell = 4.0\,\text{mm}$, $\ell_f = 6.5\,\text{mm}$, $w_f = 14.5\,\text{mm}$, $t = 1.8\,\text{mm}$, $s = 0.2\,\text{mm}$, $w_t = 18.0\,\text{mm}$, $d = 1.0\,\text{mm}$, $d_t = 7.5\,\text{mm}$, $s_x = 4.0\,\text{mm}$, and $s_y = 1.1\,\text{mm}$. (b) Side view of the fundamental antenna. (c) Antenna with Hilbert curve slit for the 5.5 GHz notched band and C-shaped slit and rectangular patch for the 3.5 GHz notched band. $c_x = 14.5\,\text{mm}$, $c_y = 5.0\,\text{mm}$, $c_w = 0.5\,\text{mm}$, $c_g = 6.0\,\text{mm}$, $c_s = 0.5\,\text{mm}$, $h_x = 6.0\,\text{mm}$, $h_y = 3.9\,\text{mm}$, $h_w = 0.5\,\text{mm}$, and $h_s = 2.5\,\text{mm}$. (d) Photograph of the dual band-notched antenna.

edge frequency is again possible with a smaller antenna size. This is equivalent to having a larger slot within the same dimension of $W_x \times W_y$, which means a lower slot resonance frequency or a wider frequency range. One can also imagine that the stub dimension d in

the y-direction has a larger impact on the resonance frequency than the dimension w_t in the x-direction. One may look into this matter from another point of view as well. At lower frequencies, the current around the slot behaves like a standing wave and the stored energy in the antenna is capacitive. The added stub increases the capacitance of the input impedance and therefore causes a lower slot resonance frequency and also a wider frequency range as its length d expands, as shown in Figure 2. However, the reflection coefficient $|S_{11}|$ over the entire band will get worse if the stub is too long. $|S_{11}|$ is not so sensitive to the width w_t as to d. The stub dimensions are finally fixed as follows: $d = 1.0$ mm and $w_t = 18$ mm.

As the dimension of the antenna is significantly reduced, the resonance frequencies arise, the spacing between two adjacent resonance frequencies increases, and the mutual coupling between neighboring resonance points decreases, which makes the intermediate impedance matching worse, especially at higher frequencies. Numerical simulation shows that the current at higher frequencies around 9 GHz concentrates between the lower edge of the slot and the feeding stub as travelling wave. It decays along the lower slot edge away from the feeding line. The two symmetrically located stubs can extend the path of current flow and decrease the current density on the ground. The stub length s_y most notably affects the resonance frequency above 9 GHz. A slight increase of s_y may shift the resonance point to an obviously lower frequency, which can be used to improve the impedance matching at higher frequencies, as illustrated in Figure 3. In order to drive the current away from its main concentration area, the distance d_t should also be long enough. However, A too large d_t may not change
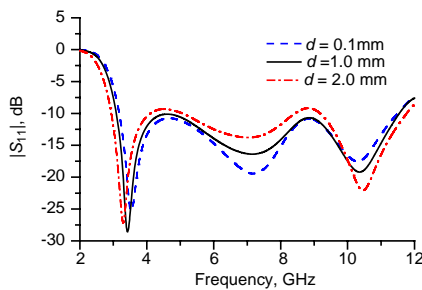

Figure 2. Simulated reflection coefficient $|S_{11}|$ with various length d of the rectangular tuning stub.
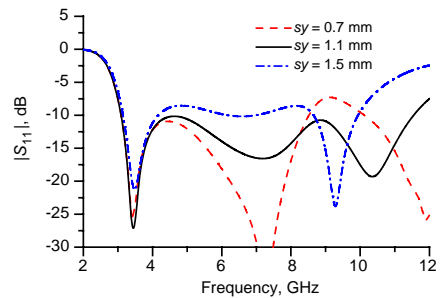
Figure 3. Simulated reflection coefficient $|S_{11}|$ with various length s_y of the symmetric stubs. $d_t = 7.5$ mm. $s_x = 4.0$ mm.

the current significantly because the current itself is relatively weak if it is located far away from the feeding line. On the other hand, the lower band performance becomes worse for a too large d_t, as shown in Figure 4. Hence a compromise should be made. The width s_x does not affect the $|S_{11}|$ much. The optimal dimensions and location of these stubs are the following: $s_x = 4.0\,\text{mm}$, $s_y = 1.1\,\text{mm}$ and $d_t = 7.5\,\text{mm}$. It can be seen from Figures 3 and 4 that the symmetric tuning stubs with optimized distance and dimensions can effectively improve the matching performance in the higher frequency band and slightly extend the lower bandwidth for electrically small length of s_y.

2.3. UWB Antennas with Dual Band-notches

Based on the fundamental structure in Figures 1(a) and 1(b), the UWB antenna with dual notched band is presented. As the original antenna without notch has already been very compact, the slit structure should be smaller in order to be integrated with it. U-shaped slits are widely used to achieve a stop band. For the 5.5 GHz notched band, the Hilbert curve slit depicted in Figures 1(c) and 1(d) is employed here as an alternative. It can be regarded as a series resonance circuit. At its resonance frequency, the current concentrates around the slit and does not radiate noticeably, which reduces the input impedance of the antenna and causes significant mismatch. Assume the lengths in the x- and y-directions equal to h_x and h_y, respectively, then the total length of the Hilbert curve slit is $h_x \times (7/3) + h_y \times (8/3)$, which is $(4/3 + 1/(3 + 6h_x/h_y))$ times of that of an U-shaped slit with the same profile $(h_x \times h_y)$. So the Hilbert curve slit can achieve the same notched band within only 3 quarters of the length of the U-shaped slit and
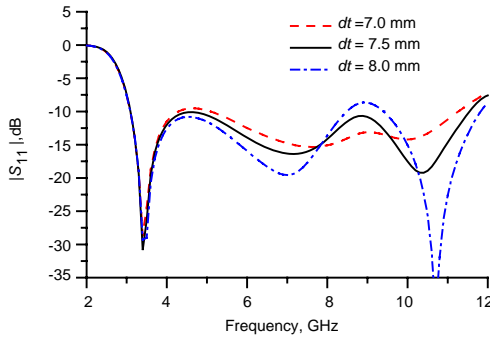

Figure 4. Simulated reflection coefficient $|S_{11}|$ with various length d_t of the symmetric stubs. $s_y = 1.1\,\text{mm}$. $s_x = 4.0\,\text{mm}$.

the stop band around 5.5 GHz can be achieved with a more compact slit structure. The parameters of the fractal slit are: $h_x = 6.0$ mm, $h_y = 3.9$ mm, $h_w = 0.5$ mm, and $h_s = 2.5$ mm. Its total length is 24.4 mm. The area occupied by the Hilbert curve pattern is 6.0 mm × 3.9 mm, which is much smaller than that by the inverted U-shaped slit of 11.9 mm × 5.0 mm if used instead. A further advantage for the slit profile reduction is that we can optimize other parameters such as h_s and h_w with more freedom.

To achieve the 3.5 GHz notched band, a C-shaped slit is etched on the upper ground plane while the slit for the 5.5 GHz band remain unchanged, as shown in Figures 1(c) and 1(d). The estimated half wavelength at 3.5 GHz is 31.7 mm. The parameters determined by simulation are $c_x = 14.5$ mm, $c_y = 5.0$ mm, $c_w = 0.5$ mm, $c_g = 6.0$ mm, $c_s = 0.5$ mm, and the total length is 33 mm. A spurious band around 10.5 GHz is observed. The related results for the antenna in Figures 1(c) and 1(d) are presented in Figure 5 and the current distribution concentrated around the C-shaped slit at 10.5 GHz is shown in Figure 6(a). It is mentioned in [12] that such kind of spurious bands is caused by the higher harmonic modes of the half or quarter wavelength slits. The central frequency of the first spurious band of a half wavelength slit is about the double of that of the first stop band. The first notched band centered at 3.5 GHz is constructed by a half wavelength slit in a symmetric way, so the slit is open in its symmetric cut plane and shorted at its two ends. Consequently, the first spurious band does not appear apparently. The central frequency 10.5 GHz of the second spurious stop band is just the triple of 3.5 GHz. This kind of phenomena is rarely or not in detail addressed in the published literature, especially regarding very compact antenna design. Hence we try a new way to eliminate the spurious stop band.
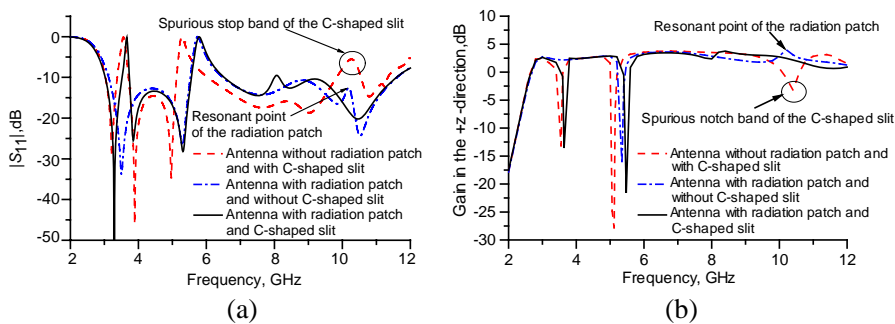

Figure 5. Effect of the rectangular patch on the spurious stop band. (a) Simulated $|S_{11}|$. (b) Simulated gain in $+z$-direction.

   As already illustrated in Figures 1(c) and 1(d), a rectangular
patch of 18.0 mm × 6.0 mm is added symmetrically on the top layer
to remove the spurious band-notch. The fundamental mode of the
patch is asymmetric and cannot be excited by the present symmetric
feeding. The second resonance frequency of the patch is at about
10.2 GHz and very close to the resonance point at 10.5 GHz of the
spurious stop band. At the frequencies of the spurious stop band, the
surface current around the slit is large due to resonance, as illustrated
in Figure 6(a). However, it does not radiate observably, which leads
consequently to significant mismatch. On the other hand, the patch is
exited to radiate effectively and compensate for the mismatch caused
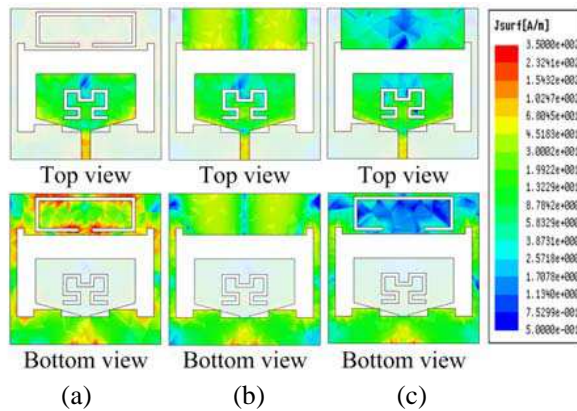by the slit, as shown in Figures 5, 6(b), and 6(c). The strong coupling

Figure 6. Current distribution at 10.5 GHz. (a) Antenna with C-shaped slit and without radiation patch. (b) Antenna with radiation patch and without C-shaped slit. (c) Antenna with C-shaped slit and radiation patch.
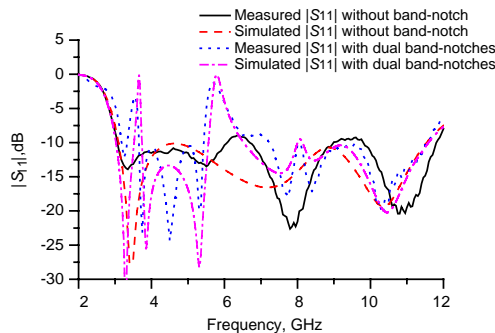

Figure 7. Comparison of measured and simulated $|S_{11}|$.

and interaction between the resonance mode of the patch and that of
the slit render the spurious band-notch to be attenuated and shifted
to a lower frequency range, as can also be seen from Figures 5 and 6.
The added patch has slight effect on the desired notch performance
at 3.5 GHz and 5.5 GHz. As the width of the patch increases, the
spurious notched band and the 3.5 GHz notched band shift slightly
to a lower frequency range, and the 5.5 GHz band shifts gradually
to a higher band. So the width of the patch should be properly
tuned to obtain optimal performance. The measured $|S_{11}|$ compared
with the simulated results for the antennas is presented in Figure 7.
It is observed that the center frequency of the spurious stop band
shifts to about 8 GHz and the corresponding mismatch decades under
acceptable level. The location of the C-shaped slit designed for the
3.5 GHz band is somewhat far away from the feeding line. The current
density around the C-shaped slit is relatively low and the amount of
stored energy there is relatively small. So the mismatch loss at 3.5 GHz
is not so high as it is at 5.5 GHz. The measured notched band centered
at 3.5 GHz is from 3.35 GHz to 3.65 GHz with $|S_{11}| > -10$ dB and that
at 5.7 GHz is from 5.3 GHz to 6.15 GHz. The results show that the
proposed antenna can reject the WiMAX and WLAN bands without
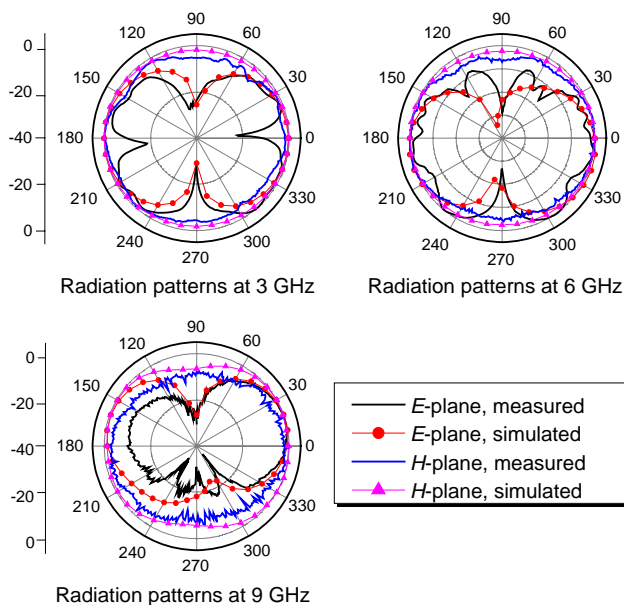spurious stop band.

Radiation patterns at 3 GHz   Radiation patterns at 6 GHz

Radiation patterns at 9 GHz

E-plane, measured
E-plane, simulated
H-plane, measured
H-plane, simulated

Figure 8. Radiation patterns for the antenna without notch.
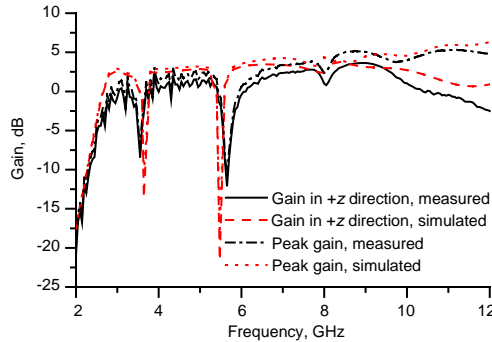
Figure 9. Measured and simulated gains for the dual band-notched antenna.

3. RADIATION PERFORMANCE

The radiation patterns are also simulated and measured in an anechoic chamber. Figure 8 depicts the simulated and measured radiation patterns for the antenna without band-notches shown in Figures 1(a) and 1(b) at frequencies of 3, 6, and 9 GHz. It is seen that the radiation concentrates in the x-z plane. The H-plane (x-z plane) patterns are generally omni-directional and become more directional with increasing frequency. The E-plane (y-z plane) patterns are roughly symmetric and have two main lobes over the entire band. However, the measured E-plane patterns have additional lobes compared with the simulated results. Since the antenna is small, the current on the outer surface of the bent coaxial cable in the measurement likely affects the radiation patterns, which has not been taken into account in the simulation model. The radiation patterns for the dual band-notched antenna are similar to those for the original antenna without any notch, except that the dual notched antenna does not radiate significantly at and near the notch frequencies. Both the peak gain and gain in the $+z$-direction for the antenna with dual band-notches are measured and given in Figure 9. As the frequency increases, the antenna becomes more directional and the peak gain increases. However, the main lobe shifts away from the $+z$-direction, which causes a decreased gain at high frequencies in that direction.

4. CONCLUSIONS

A very compact wide slot UWB antenna with dual band-notched function is presented with simulated and measured results. Parametric

studies have been done to find out the optimal dimensions of the stubs and resonance structures. Different slit structures have been investigated to achieve the desired band-notched characteristics. The spurious notched band has been studied in detail and its influence eliminated effectively by adding a patch resonating and radiating in the same frequency range to compensate for the mismatch caused by the non-radiating slit.

ACKNOWLEDGMENT

REFERENCES

1. Dissanayake, T. and K. P. Esselle, "UWB performance of compact L-shaped wide slot antennas," *IEEE Trans. Antennas Propag.*, Vol. 56, No. 4, 1183–1187, 2008.

2. Dong, Y. D., W. Hong, Z. Q. Kuai, C. Yu, Y. Zhang, J. Y. Zhou, and J.-X. Chen, "Development of ultrawideband antenna with multiple band-notched characteristics using half mode substrate integrated waveguide cavity technology," *IEEE Trans. Antennas Propag.*, Vol. 56, No. 9, 2894–2902, 2008.

3. Sze, J.-Y. and J.-Y. Shiu, "Design of band-notched ultrawideband square aperture antenna with a hat-shaped back-patch," *IEEE Trans. Antennas Propag.*, Vol. 56, No. 10, 3311–3314, 2008.

4. Zhou, H.-J., B.-H. Sun, Q.-Z. Liu, and J.-Y. Deng, "Implementation and investigation of U-shaped aperture UWB antenna with dual band-notched characteristics," *Electron. Lett.*, Vol. 44, No. 24, 1387–1388, 2008.

5. Qing, X. and Z. N. Chen, "Compact coplanar waveguide-fed ultrawideband monopole-like slot antenna," *IET Microw. Antennas Propag.*, Vol. 3, No. 5, 889–898, 2009.

6. Ye, L.-H. and Q.-X. Chu, "3.5/5.5 GHz dual band-notch ultrawideband slot antenna with compact size," *Electron. Lett.*, Vol. 46, No. 5, 325–327, 2010.

7. Li, W.-M., T. Ni, S.-M. Zhang, J. Huang, and Y.-C. Jiao, "UWB printed slot antenna with dual band-notched characteristic,"

Progress In Electromagnetics Research Letters, Vol. 25, 143–151, 2011.

8. Taheri, M. M. S., H. R. Hassani, and S. M. A. Nezhad, "UWB printed slot antenna with bluetooth and dual notch bands," *IEEE Antennas Wireless Propag. Lett.*, Vol. 10, 255–258, 2011.

9. Ma, T.-G. and S.-J. Wu, "Ultrawideband band-notched folded strip monopole antenna," *IEEE Trans. Antennas Propag.*, Vol. 55, No. 9, 2473–2479, 2007.

10. Abbosh, A. M. and M. E. Bialkowski, "Design of UWB planar band-notched antenna using parasitic elements," *IEEE Trans. Antennas Propag.*, Vol. 57, No. 3, 796–799, 2009.

11. Liu, W. X. and Y. Z. Yin, "Dual band-notched antenna with the parasitic strip for UWB," *Progress In Electromagnetics Research Letters*, Vol. 25, 21–30, 2011.

12. Dong, Y. D., W. Hong, Z. Q. Kuai, and J. X. Chen, "Analysis of planar ultrawideband antennas with on-ground slot band-notched structures," *IEEE Trans. Antennas Propag.*, Vol. 57, No. 7, 1886–1893, 2009.

13. Ryu, K. S. and A. Kishk, "UWB antenna with single or dual band-notches for lower WLAN band and upper WLAN band," *IEEE Trans. Antennas Propag.*, Vol. 57, No. 12, 3942–3950, 2009.

14. Ren, L.-S., F. Li, J.-J. Zhao, G. Zhao, and Y.-C. Jiao, "A novel compact UWB antenna with 3.5/5.2/5.8 GHz triple band-notched characteristics," *Progress In Electromagnetics Research Letters*, Vol. 16, 131–139, 2010.